Preprints of the 21st IFAC World Congress (Virtual)
Berlin, Germany, July 12-17, 2020

TDLAS/WMS Embedded System for Oxygen Concentration Detection of Glass Vials with Variational Mode Decomposition

Qiwu Luo, Chunhua Yang*, Cao Song, Jian Zhou, Weihua Gui

*School of Automation, Central South University, Changsha, Hunan Province, China, 410083, (Tel: +86 0731 88830700; *e-mail: ychh@ csu.edu.cn).*

Abstract: Whether the oxygen content for medical glass vials can be measured accurately affects greatly the ingredient stability of sterile pharmaceuticals. Tunable diode laser absorption spectroscopy (TDLAS/WMS) based on wavelength modulation has the remarkable advantages of non-contact, low cost, high sensitivity, real-time response, which shows great potential in the field of in-site oxygen concentration detection. Due to the short optical path and various environmental disturbances, it is challenging to measure the headspace oxygen concentration in open-path optical environment. Targeting this challenge, this paper designs a TDLAS/WMS-based gas concentration sensing architecture and turns it into an embedded detection system. Then, a robust signal reconstruction method based on variational mode decomposition (VMD) is established to suppress the random noise of the demodulated harmonic signal. Hence, the oxygen concentration can be reliably inversed from the peak-to-peak values (V_{p-p}) of the 2nd harmonic signal. This detection framework is abbreviated as WMS+VDM+V_{p-p}. Encouragingly, the preliminary application on a glass vial encapsulation line demonstrate that the proposed method performs promising results with an absolute detection error of within ±1.5% and a minimal Allan deviation of 0.0010@(100s), which provides a good start for the on-site headspace oxygen concentration measurement for pharmaceutical glass vials.

Keywords: Oxygen concentration detection, glass medicine vials, wavelength modulation spectroscopy (WMS), variational mode decomposition (VMD), signal reconstruction, open-path optical environment.

1. INTRODUCTION

Evacuation or nitrogen-filling is widely applied in the encapsulation of glass medicine vials to preserve the medicine ingredients from being oxidized. Unfortunately, on account of the unsteady capping, the sterile product container-closure would be unavoidably broken, so achieving the online detection of oxygen concentration in glass medicine vials during the encapsulation process has been recently attracting considerable attentions. Recently, tunable diode laser absorption spectroscopy based on wavelength modulation (TDLAS /WMS) (Arndt (1965)) enjoys the increasing popularity in trace gases online detection (Lan *et al.* (2019a, b)), which has the characteristics of the extremely narrow spectral line width, low cost, high sensitivity, nondestructive and real-time response. Unfortunately, nearly all the technique roadmaps in recent references resort to either multiple costly instruments or confined gas absorption cells (Lan *et al.* (2019b)), while the pharmaceutical automation industry expects cost-effective and compact detection devices for enhance the product competitiveness.

Under the above application trends, most pharmaceutical manufacturers attempt to realize the online detection of oxygen concentration without changing the existing production line infrastructures and production procedures. For most glass vial packaging line, the headspace oxygen detection process can be accommodated on the rotating platform of the automated visual inspection (AVI) machine (refer to Fig. 2). However, the side effect is that the measurement of headspace oxygen concentration needs to be operated in open-path optical environment in real time, and the available installation space is still limited. Owing to the short optical path and various environmental disturbances, it is an extremely intractable task. Consequently, the demodulated 2nd harmonic signals by using TDLAS/WMS are always struggling to survive in multiple complex noises. So then, the engineering task of in-site oxygen concentration detection is transformed into a signal reconstruction problem from noise-polluted 2nd harmonic signals.

Recently, some signal filtering methods are designed for gas content detection in TDLAS system. A totally adaptive Savitzky-Golay filtering method was proposed for infrared gas detection by using the least squares fitting coefficients response function (Li *et al.* (2015)). And cubic spline interpolation method is used to fit the absorption spectrum in (Wang *et al.* (2017)). However, the stochastic noises are always distributed randomly among each frequency band while the above methods refine the absorption spectrum signal in only time domain. Further, some spectral transform methods are imported for noise suppression. The empirical mode decomposition (EMD) (Yang *et al.* (2017)) has been applied on the signal reconstruction of 2nd harmonic signal in TDLAS system (Meng *et al.* (2014)). But the EMD has been reported to be easy to generate mode aliasing, and its mathematical theory basis is also limited. Fortunately, a new framework of variational mode decomposition (VMD)

(Dragomiretskiy *et al.* (2014)) is generalized from EMD with adaptive bands restriction by multiple classic Wiener filters. The VMD provides a decomposition solution and its theory is also easy to be understood. Many application cases utilizing the VMD can be available in recent references. (Wang *et al.* (2015)) proposed a method of rubbing fault diagnosis based on VMD. And the detrended fluctuation analysis (DFA) combined with VMD was used to robustly address signal denoising problem (Liu *et al.* (2016)).

In this paper, we investigate that the VMD is promising in denoising the demodulated 2nd harmonic signals in TDLAS system. A detection scheme of WMS+VDM+V_{p-p} is founded where the headspace oxygen content can be readily but stably inversed from the peak-to-peak values of the 2nd harmonic signals. The primary contributions are as follows.

1) A VMD-based 2nd harmonic filter algorithm is proposed to effectively suppress the complex random noises. The adaptable parameter configurations, for instance, frequency segment layers and cross-correlation coefficients are measured and analysed carefully.

2) A TDLAS/WMS prototype is implemented on a set of modular embedded circuit boards. It is successfully applied on an AVI machine to detect headspace oxygen concentration of penicillin vials, which provides a preliminary reference case for TDLAS/WMS study.

3) The precision and stability of the proposed method of WMS+VDM+V_{p-p} is verified on our designed TDLAS/WMS embedded system through a series of comparison tests and Allan variance analysis.

The structure of this paper is as follows. Section 2 imports the theoretical basis of TDLAS/WMS. Section 3 illustrates the experiment setup and the challenges of application. Our methodology process and the associated parameter settings are elaborated in Section 4. Further in Section 5, a series of actual comparison experiments are implemented and the stability and precision of the proposed prototype are evaluated by the Allan variance analysis. Finally, we conclude this paper in Section 6.

2. TDLAS/WMS

Our previous work (Luo *et al.* (2019) and Axner *et al.* (2001)) on TDLAS/WMS has proved the relationship between the maximum amplitude (i_{2fmax}) and the absorption gas concentration N, as follow:

$$N = \frac{i_{2f\max}}{4i_0^p|_{\nu_c=\nu_0}} \frac{\pi \Delta\nu_c m^2}{s(T)LP} \left[\frac{2-\left(2+m^2\right)}{\sqrt{(1+m^2)}} \right]^{-1} \quad (1)$$

where $s(T)$ represents the spectral feature line strength, T is the environment temperature, L stands for the absorption optical length, P is the pressure of the absorption gas. $\Delta\nu_c$ denotes the full width at half maximum of Lorentzian line shape, m is the frequency modulation degree. It is worth mentioning that, in real-world application, i_{2fmax} is sometimes replaced by the V_{p-p} of the 2nd harmonic signal to ensure the higher concentration inversion precision.

3. EXPERIMENT DETAILS AND CHALLENGES

According to the theory reviewed above, as shown in figure 1, we design a TDLAS/WMS oxygen concentration detection scheme. As shown in Fig. 2, this detection scheme

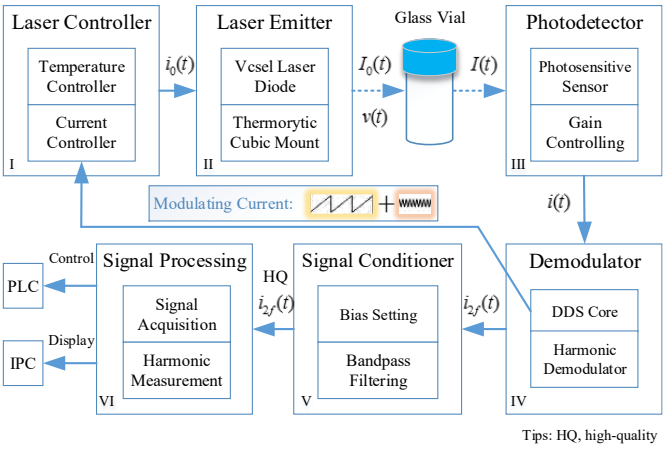

Fig. 1. Oxygen concentration sensing framework based on TDLAS/WMS.

Fig. 2. The TDLAS/WMS prototype photo and testing scene, taken at the Truking Academician Workstation.

is realized and then applied on an AVI machine for headspace oxygen concentration detection of penicillin vials. It has been shown in many applications that the wavelength of laser light to a target can be precisely adjusted by temperature and/or current variations. Here on and off the O_2 absorption, which is around 760 nm. The laser emitter (II) conducts at a stationary temperature in conjunction with the laser controller (I), and its current controller is controlled by the DDS core of the demodulator (IV), which generates a modulated current to actuate the laser diode. The photodetector (III) gathers the transmission intensity of the laser beams traveling through the open-path optical path, which is harmonic demodulated in the digital demodulator (IV), then the depressed spectrum absorbed by O_2 can be extracted. The band-limited signal regulator (V) amplifies the weak 2nd-harmonic signal after demodulation, setting the bandwidth to 0.01Hz ~ 150Hz for noise-robustness reduction. Feature extraction and calculation are completed by signal processing unit (VI), which is a key factor in oxygen concentration retrieval and medical glass vial qualification determination. PLC controls the corresponding transmission device according to the decision-making results, positioning the glass bottles with different qualities to corresponding

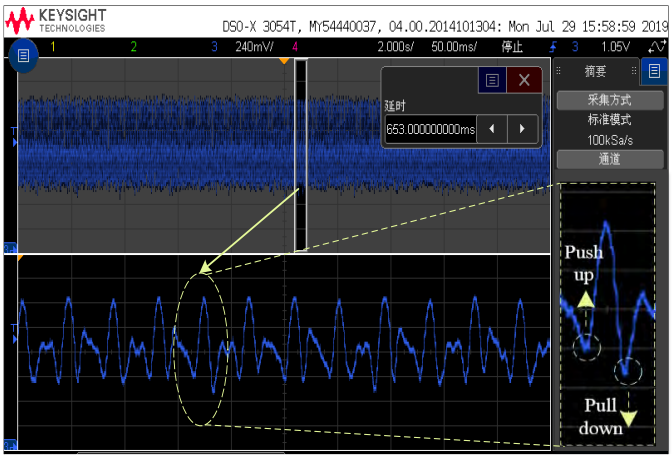

Fig. 3. Signal distortion resulted from stochastic noises.

transmission channels. Finally, a measuring interface exists on IPC, completing backup and data analysis simultaneously.

In this experiment, the test samples are *four* sets of pelicillin bottles with well differentiated oxygen concentration values of 0%, 5%, 10% and 21%, respectively, and each glass vial is tested for 15 min, then the 22500 of 2nd-harmonic signals are obtained. As shown in Fig. 3, each 2nd harmonic is randomly gathered from our embedded detection system of oxygen concentration. It is clearly observed that the valley value of left side-lobe is lower than that of the right side-lobe, the appearance of each cycle is distinct, and the whole signal envelope is slightly fluctuated. It should be pointed out that the weak second harmonic signal, which is not smooth and asymmetric in the left and right valley, is affected by a variety of optics noise and random electronic noises. If it is directly used in the inversion of oxygen concentration, the detection result will be incorrect. This problem is very challenging, which is the exactly focus of this paper. We propose a method of signal reconstruction based on VMD. The analysis and processing of this method will be introduced in section 4.

4. METHODOLOGY AND ANALYSIS

The operation process of the signal reconstruction based on VMD can be categorized into three main steps. First, the original 2nd-harmonic f is decomposed into all possible intrinsic mode functions (IMFs (the specific definition can be referred to (Huang *et al.* (1998)))). Second, the cross-correlation coefficients C_i between f and IMFs can be gained by cross-correlation operation, respectively. Third, the filtered 2nd harmonic signal can be reconstructed from the multiplicative sum of IMFs and the corresponding cross-correlation coefficients C_i. Here are the detailed steps:

Step 1. The centre frequency of each mode is initially divided (the specific process can be referred to (Wang *et al.* (2015))) by structuring the constrained variational problem

$$\min_{\{u_k\},\{\omega_k\}}\left\{\sum_k\left\|\partial_t\left[\left(\delta(t)+\frac{j}{\pi t}\right)*u_k(t)\right]e^{-j\omega_k t}\right\|_2^2\right\}\qquad s.t.\sum_k u_k=f \quad (2)$$

where $\{u_k\}$ represents the shorthand notations for the set of all modes, $\{\omega_k\}$ represents the centre frequencies. We take the raw 2nd harmonic of glass vial with oxygen concentration of 0% for illustration, which are segmented into 8 segments. Particularly in this paper, the corresponding initial centre frequencies are 0, 0.0024π, 0.0196π, 0.0589π, 0.0708π, 0.3401π, 0.3911π, 0.4248π, respectively.

Step 2. A quadratic penalty term a and Lagrangian multipliers λ are introduced to render the constrained variational problem unconstrained

$$\begin{aligned}L(\{u_k\},\{\omega_k\},\lambda)=a\sum_k\left\|\partial_t\left[\left(\delta(t)+\frac{j}{\pi t}\right)*u_k(t)\right]e^{-j\omega_k t}\right\|_2^2\\+\left\|f-\sum_k u_k(t)\right\|_2^2+\left\langle\lambda(t),f-\sum_k u_k(t)\right\rangle\end{aligned} \quad (3)$$

where a is closely related to the reconstruction fidelity. For big a (*e.g.* set to 50), two or more different modes share the main parts of the signal. For small a (*e.g.* set to 1), one or several additional modes are mainly composed of noise, therefore, the spectral density becomes broad. What needs to be pointed out is that the quadratic penalty term a is set to 10 for compromise in this paper.

Step 3. The centre frequency ω_k and bandwidth of each mode u_k are iterated L times until to satisfy the accuracy requirement $\sum_k\|u_k^{n+1}-u_k^n\|_2^2/\|u_k^n\|_2^2<\varepsilon$. The iteration expressions are as follows

$$\hat{u}_k^{n+1}(\omega)=\frac{\hat{f}(\omega)-\sum_{i\neq k}\hat{u}_i(\omega)+\frac{\hat{\lambda}(\omega)}{2}}{1+2a(\omega-\omega_k)^2} \quad (4)$$

$$\omega_k^{n+1}=\frac{\int_0^\infty\omega\left|\hat{u}_k(\omega)\right|^2d\omega}{\int_0^\infty\left|\hat{u}_k(\omega)\right|^2d\omega} \quad (5)$$

Particularly in this paper, a total of 500 iterations are performed to obtain the 8 modes of u_k. The corresponding centre frequencies are learnt as 0, 0.0380π, 0.0859π, 0.0101π, 0.1526π, 0.3130π, 0.2163π, 0.4392π, respectively. The decomposed results of the 2nd-harmonic signal are presented in Fig. 4.

Step 4. The cross-correlation coefficients C_i between f and modes u_k are calculated by using cross-correlation operation

$$C_i=\lim_{T\to\infty}\frac{1}{T}\int_0^T f\bullet u_k dt \quad (6)$$

where T represents the duration of the signal f. Particularly in this paper, the duration discrete time is set to 500.

Step 5. The reconstructed 2nd-harmonic signal f' can be obtained from the multiplicative sum of u_i and C_i by turn

$$f'=\sum_{i=1}^k C_i\bullet u_i \quad (7)$$

After completing from the Step 1 through 5, we can gain the reconstructed 2nd harmonic signal (refer to Fig. 5), in which the stochastic noises are robustly suppressed with an almost symmetric envelope. In addition, the amplitude attenuation can be insignificant. Particularly in this paper, the correlation coefficients C_1 to C_8 evaluated in (11) are 0.9926, 0.4020, 0.2307, 0.7636, 0.2279, 0.0298, 0.0116, 0.0200, respectively. It indicates that, the closer the centre frequency of each mode is to the low frequency, the more relevant the

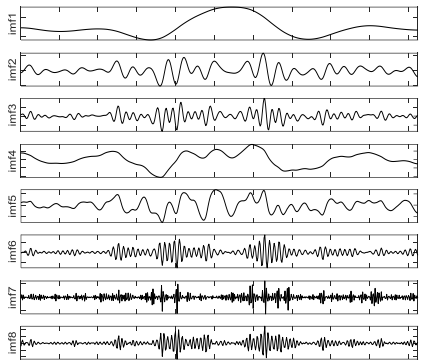

Fig. 4. Signal distortion resulted from stochastic noises.

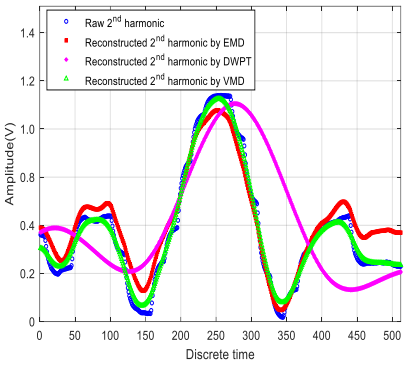

Fig. 5. Comparison reconstruction effects by using methods of EMD, DWPT and VMD.

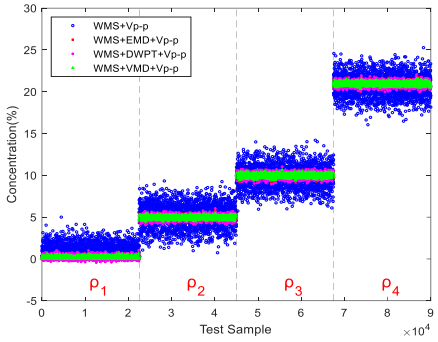

Fig. 6. Detection results using the four competitive schemes for one full hour. (ρ_1, ρ_2, ρ_3, ρ_4 stands for glass vials with the oxygen concentration of 0%, 5%, 10%, 21%, respectively.)

mode is to the original 2nd harmonic signal. So, the principal components in raw 2nd harmonic signal can be adaptively enhanced and other nonsignificant components can be weakened by reconstruction couple with cross-correlation operation. Further, it is obvious from Fig. 5, when using traditional EMD method, the amplitude of the reconstructed signal drops slightly than that of VMD, and the signal envelope is still not so symmetric. The main reason is that the inter-mode aliasing problem of EMD might lead to principle feature loss. Furthermore, the DWPT method used in (Luo *et al.* (2019)) is used for comparison, the reconstructed 2nd harmonic signal based on DWPT using Coiflet5 function performs smoothness well, but the left and right valleys of the reconstructed signal are not equal. Therefore, the universality of the DWPT for all signals needs to be improved.

5. EXPERIMENTAL RESULTS AND DISCUSSION

5.1 Detection Precision Evaluation

Here the experimental configurations in the section 3 are fully inherited in this section for oxygen concentration detection of penicillin vials for evaluating the precision of our proposed method of WMS+VMD+V_{p-p}. The fundamental scheme inversing oxygen concentration directly from the V_{p-p} of the 2nd-harmonic signal is chosen as the baseline, which is denoted as 'WMS+V_{p-p}'. And the VMD is replaced by its further operator EMD, then another competitive detection schemes of WMS+EMD+V_{p-p} and WMS+DWPT+V_{p-p} are involved to carry out. For a fair comparison, a series of 2nd-harmonic signals are captured by the TDLAS/WMS embedded system, and then we use these same data to evaluate the effect of the four comparison methods. Fig. 6 shows the concentration measurement results after 22500 rounds of continuous tests for each test group. It is obvious that the scheme of WMS+VMD+V_{p-p} performs better than that based on EMD and DWPT, while the adjacent detection results using the WMS+ Vp-p basic scheme tend to overlap many cases, which will be sure to trigger false or missed detection. For more insight understanding, the indicators of absolute error are listed in the Table 1. As we can see, the total absolute error achieved by the scheme of WMS+VMD+V_{p-p} is within -1.51% to 1.50%. In contrast, the detection error range of the scheme of WMS+EMD+V_{p-p} varies from -2.15% to 2.13% and the scheme of WMS+DWPT+V_{p-p} varies from -2.20% to 2.09%. Moreover, the baseline scheme of WMS+V_{p-p} experiencing the most violent fluctuations in Fig. 6 suffers the worst absolute error range of -5.21%~5.02%. Not surprisingly, some test samples (*e.g.*, concentration ρ_1) are even mistakenly identified their concentration as 5%. And the main reason for this result is that the decision criteria of V_{p-p} is easily affected by many noises in actual industrial applications. Any noise in the peak or the valleys will lead to the error of V_{p-p} value, which is easy to cause misjudgment. Further, the measurement accuracy of WMS + EMD + Vp-p scheme has been improved to a large extent. However, the inherent problem of generating mode aliasing makes this method survive hard in harsh industrial environment. In addition, the performance of this method of WMS+DWPT+V_{p-p} can not perform the best one due to the lack of adapting to the all noises superimposed on the 2nd harmonics. The preliminary performance yielded by WMS+VMD+V_{p-p} scheme proves that the VMD works better than EMD and DWPT in anting complex noises in open-path optical condition.

5.2 System Stability Analysis

Allan variance analysis (Werle *et al.* (1993)) is one of the most commonly used methods to identify and quantify the noise items in inertial sensor data, which can be used to determine the function that the integrating time is replaced with the inevitable noise of the system. Hence the Allan variance analysis is imported to evaluate the detection stability of our embedded system by using the three different methods. The analysis results corresponding to the four test groups in Fig. 6 are given in Fig.7, Fig.8, Fig.9 and Fig.10. When the slope of the dotted line is -0.5 (dashed line), the white noise dominates. The optimum integrating time (τ_{opt}) and the lower detection limit are determined by the minimum σ_{Allan} ($\sigma_{Allan(min)}$). The experimental results show that the detection accuracy of WMS+VMD+ V_{p-p} scheme is higher than that of the other three methods in the range of white noise and brown noise. For example, the σ_{Allan} using the methods of WMS+V_{p-p}, WMS+EMD+V_{p-p}, WMS+DWPT+V_{p-p} and WMS+VMD+V_{p-p} at 10s for test samples with concentration of 0% are 0.0391, 0.0106, 0.0134 and 0.0081, respectively, proving again that our scheme can suppress the random noises most effectively. More detailed performance

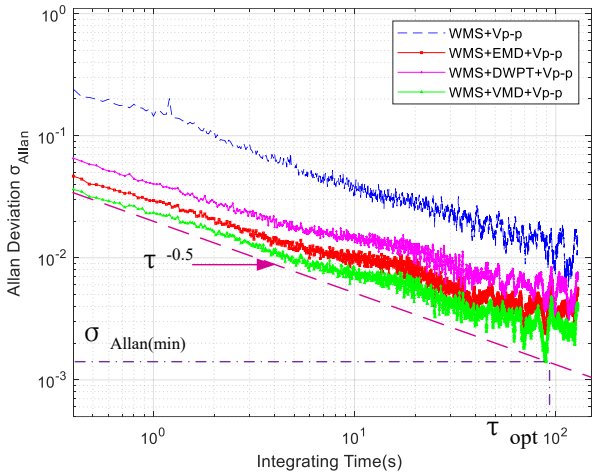

Fig.7. Allen charts of four schemes - standard medical glass bottle for 0% concentration of oxygen.

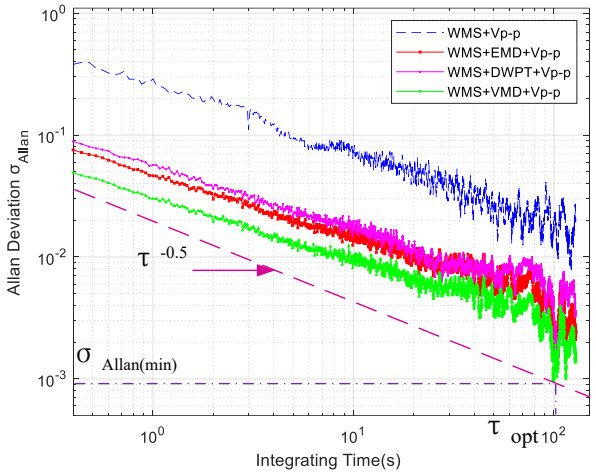

Fig.8. Allen charts of four schemes - standard medical glass bottle for 10% concentration of oxygen..

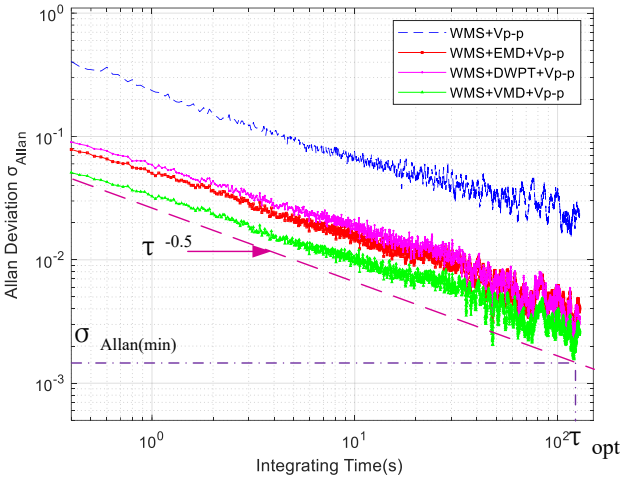

Fig.9. Allen charts of four schemes - standard medical glass bottle for 5% concentration of oxygen.

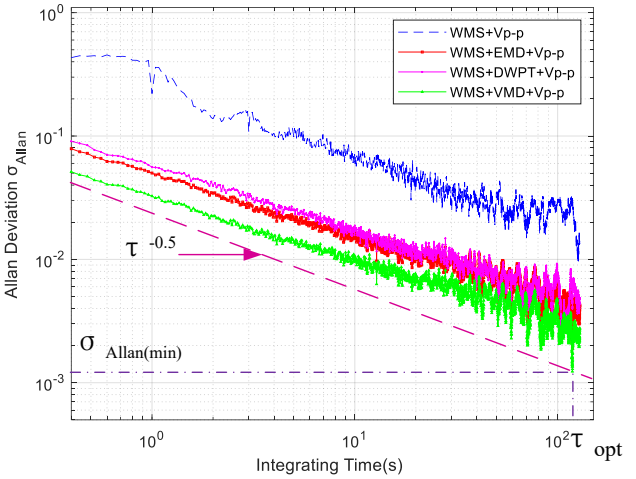

Fig.10. Allen charts of four schemes - standard medical glass bottle for 21% concentration of oxygen.

judged by σ_{Allan} for *four* kinds of test samples with *four* methods can be available in the Table 1. As expected, our scheme of WMS+VMD+V_{p-p} can obtain the lowest $\sigma_{Allan(min)}$ in any case. The essential reason is that the VMD-based detection scheme can realize completely non- recursive and adaptive noise suppression, the effective signal separation ability in frequency domain promotes our oxygen detection method to achieve the satisfactory precision and reliability on our realized embedded system.

6. CONCLUSION

This work concentrates on how to robustly denoise the demodulated harmonic signals on the TDLAS/WMS sensing system in order to provide a reliable solution for the realization of in-site headspace oxygen concentration in the field of medical glass bottles in the industrial open-path optical environment. Inspired by the spectrum shifting concept of WMS, the multiple random noises are effectively tracked by VMD from a sets of filter arrays with narrow bandwidth and adaptively tunable centre frequencies. With the well reconstructed 2nd harmonic signals, an oxygen measurement scheme of WMS+VDM+V_{p-p} is raised based on lightweight concentration inversion by peak-to-peak values. The whole methodology has been realized on embedded circuits and then been applied on an AVI machine. The application effects show that our presented method has a good application prospect both on the detection stability and precision. Till now, our system has been running stably for more than six months in the workshop at *Truking Tech.*, which offers a good beginning for the industrial application of online and precise residual oxygen detection for glass packaged medicine.

ACKNOWLEDGMENT

This work was jointly funded by the National Natural Science Foundation of China under Grant 61973323, Grant 51704089 and Grant 61873282, and the Anhui Provincial Natural Science Foundation of China under Grant 1808085QF190.

The authors would like to express their gratitude to Mr. Jianping Zhu and Ms. Shujie Li, respectively a senior engineer and the HoD of AVI department in *Truking Tech.*, who helped verify the performance of the prototype for this paper.

Table 1. *The absolute error and Allen variance analysis of four comparison detection methods.*

Concentration	Methods	Absolute error	σ_{Allan}@10s	$\sigma_{Allan(min)}$@τ_{opt}(s)
0%_oxygen	WMS+V_{p-p}	0% ~ 5.00%	0.0391	0.0057@(115s)
	WMS+EMD+V_{p-p}	0% ~ 1.98%	0.0106	0.0022@(69s)
	WMS+DWPT+V_{p-p}	0% ~ 2.01%	0.0134	0.0039@(87s)
	WMS+VMD+V_{p-p}	0% ~ 1.50%	0.0081	0.0014@(89s)
5%_oxygen	WMS+V_{p-p}	-4.99% ~ 4.98%	0.0745	0.0077@(122s)
	WMS+EMD+V_{p-p}	-2.02% ~ 2.01%	0.0135	0.0015@(99s)
	WMS+DWPT+V_{p-p}	-2.20% ~ 2.03%	0.0166	0.0023@(97s)
	WMS+VMD+V_{p-p}	-1.46% ~ 1.49%	0.0088	0.0010@(100s)
10%_oxygen	WMS+V_{p-p}	-5.21% ~ -4.89%	0.0735	0.0154@(116s)
	WMS+EMD+V_{p-p}	-1.97% ~ 2.13%	0.0142	0.0024@(119s)
	WMS+DWPT+V_{p-p}	-1.99% ~ 2.09%	0.0174	0.0022@ (122s)
	WMS+VMD+V_{p-p}	-1.51% ~ 1.46%	0.0093	0.0016@(120s)
21%_oxygen	WMS+V_{p-p}	-4.14% ~ 5.02%	0.0698	0.0097@(126s)
	WMS+EMD+V_{p-p}	-2.15% ~ 2.03%	0.0164	0.0018@(117s)
	WMS+DWPT+V_{p-p}	-2.04% ~ 2.01%	0.0188	0.0020@(105s)
	WMS+VMD+V_{p-p}	-1.42% ~ 1.43%	0.0107	0.0012@(118s)

REFERENCES

Arndt R. (1965). Analytical line shapes for Lorentzian signals broadened by modulation. *Journal of Applied Physics*, 36(8), 2522-2524.

Axner O., Kluczynski P. and Lindberg A.M. (2001). A general non-complex analytical expression for the nth Fourier component of a wavelength-modulated Lorentzian lineshape function. *Journal of Quantitative Spectroscopy & Radiative Transfer*, 68(3), 299-317.

Dragomiretskiy K. and Zosso D. (2014). Variational mode decomposition. *IEEE Transactions on Signal Processing*, 62(3), 531-544.

Li J., Deng H., *et al*. (2015). Real-time infrared gas detection based on an adaptive Savitzky-Golay algorithm. *Applied Physics B: Lasers and Optics*, 120(2), 207-216.

Lan L., Chen J., Zhao X., and Ghasemifard H. (2019). VCSEL-based atmospheric trace gas sensor using first harmonic detection. *IEEE Sensors Journal*, 19(13), 4923-4931.

Lan L., Chen J., Wu Y., Bai Y., Bi X., and Li Y. (2019). Self-calibrated multiharmonic CO_2 sensor using VCSEL for urban in situ measurement. *IEEE Transactions on Instrumentation and Measurement*, 68(4), 1140-1147.

Liu Y., Yang G., Li M. and Yin H. (2016). Variational mode decomposition denoising combined the detrended fluctuation analysis. *Signal Processing*, 125, 349-364.

Meng Y., Liu T., Liu K., Jiang J., Wang R., Wang T., and Hu H. (2014). A modified empirical mode decomposition algorithm in TDLAS for gas detection. *IEEE Photonics Journa*l, 6(6), 1-7.

Wang Y., Markert R., Xiang J., and Zheng W. (2015). Research on variational mode decomposition and its application in detecting rub-impact fault of the rotor system. *Mechanical Systems and Signal Processing*, 60, 243-251.

Wang Y., Wei Y., Chang J., Zhang T., Liu T., Sun T., and Grattan K. T. (2017). Tunable diode laser absorption spectroscopy- based detection of propane for explosion early warning by using a vertical cavity surface enhanced laser source and principle component analysis approach. I *IEEE Sensors Journal*, 17(15), 4975-4982.

Yang X., Yue H. and Ren J. (2017). Fuzzy empirical mode decomposition for smoothing wind power with battery energy storage system. *IFAC2017,* 50(1), 8769-8774.

Q. Luo, C. Song, C. Yang, W. Gui, et al. (2019), Headspace oxygen concentration measurement for pharmaceutical glass vials in open-path optical environment using TDLAS /WMS. *IEEE Trans. Instrum. Meas*., DOI: 10.1109/TIM.2019.2958582, Dec. 2019.

Huang. N. E, Shen. Z, Long. S. R, et al., "The empirical mode decomposition and the Hilbert spectrum for nonlinear and non-stationary time series analysis,". *Proceedings A*, vol.454, no.1, pp.903-995, 1998.

P. Werle, R. Mucke and F. Slemr, The Limits of Signal Averaging in Atmospheric Trace-Gas Monitoring by Tunable Diode-Laser Absorption Spectroscopy (TDLAS). Appl. Phys. B, vol. 57, pp.131-139, Apr. 1993.